applied sciences

MDPI

Article

Identifying Fatigue Behaviors of Asphalt Mixture Under Different Strain Waveforms, Temperatures and Rest Periods with Dissipated Energy Method

Yu Cai [1], Xiangping Wang [2], Huailei Cheng [3,*], Jia Guo [2], Mingjun Hu [4] and Lijun Sun [3]

[1] Zhangji Expressway Reconstruction and Expansion Project Office of Jiangxi Provincial Transportation Investment Group Co., Ltd., Nanchang 330000, China
[2] Hebei Transportation Investment Group Hengde Expressway Co., Ltd., Shijiazhuang 050000, China
[3] The Key Laboratory of Road and Traffic Engineering Ministry of Education, Tongji University, Shanghai 201804, China
[4] School of Infrastructure Engineering, Dalian University of Technology, Dalian 116024, China
* Correspondence: chl6218@tongji.edu.cn

Abstract

Fatigue behaviors in asphalt mixtures are influenced by multiple factors, including strain level, strain waveform, and temperature, as well as rest periods. This complexity makes the analysis and interpretation of fatigue data particularly challenging. Dissipated energy (DE) is effective for developing unified fatigue models that characterize asphalt mixture behavior across varying temperatures and strain levels. However, its applicability requires further validation across a broader range of loading scenarios, especially those involving diverse strain waveforms and rest periods. This research aimed to apply the dissipated energy method to analyze fatigue behaviors of asphalt mixture subjected to extended combinations of strain waveforms and temperatures, as well as rest periods. It was found that strain waveform significantly impacts DE values and the rate of DE variation in asphalt mixtures, which contributes to differences in fatigue life at varying strain waveforms. The initial DE (IDE) indicator establishes a distinct correlation with the fatigue life of the asphalt mixture, unaffected by strain waveforms or strain levels. However, this IDE-fatigue life relationship is influenced by rest periods and temperatures. Longer rest periods shift the IDE-fatigue life curve toward a higher fatigue life, indicating improved performance. Through IDE analysis, a generalized model was formulated to represent IDE-fatigue life relationships across broad strain waveforms and strain levels, as well as rest periods, facilitating fatigue life prediction under changing conditions. This research provides valuable insights into the fatigue characteristics and underlying mechanisms of asphalt mixtures from an energy perspective.

Keywords: asphalt mixture; fatigue behavior; strain waveform; temperature and rest period; dissipated energy

Check for updates

Academic Editor: Luís Picado Santos

Received: 14 January 2026
Revised: 4 February 2026
Accepted: 12 February 2026
Published: 21 February 2026

Copyright: © 2026 by the authors. Licensee MDPI, Basel, Switzerland. This article is an open access article distributed under the terms and conditions of the Creative Commons Attribution (CC BY) license.

1. Introduction

Fatigue performance represents a crucial property of asphalt mixtures, as it predominantly influences the resistance to fatigue cracking within the pavement structure [1–4]. Understanding fatigue behaviors of asphalt mixture provides essential insights for evaluating their fatigue performance. To investigate these behaviors, fatigue tests are commonly conducted to measure key response parameters such as stiffness modulus and

phase angle [5–7]. With the collected response data, fatigue life and damage mechanisms of the mixture can be analyzed to assess its performance under repeated loading.

In service, asphalt mixture layers are exposed to varying temperatures and vehicle loading conditions. To replicate these real-world factors, fatigue tests have been conducted under different temperature and loading scenarios. For instance, previous studies have investigated the fatigue characteristics of asphalt mixtures at temperatures ranging from below 0 °C to over 35 °C. These studies have shown that fatigue responses, such as stiffness modulus and fatigue life, are highly temperature-dependent [8,9]. This temperature sensitivity can largely be attributed to the viscoelastic properties of asphalt mixtures: as temperature increases, the mixture's resistance to elastic deformation decreases, while its viscous behavior intensifies [10–12].

In fatigue testing of asphalt mixtures, variations in loading levels, waveforms, and rest periods are considered to better simulate real-world conditions. The loading level represents the magnitude of strain or stress in each cycle and aims to mimic the different axle load levels encountered in truck traffic. Generally, as the loading level increases, the mixture's fatigue life decreases [13,14]. Strain waveforms describe the shape of the load pulses during each cycle. Conventional waveforms, such as haversine and sinusoidal waves, are commonly used in fatigue tests due to their ease of implementation. However, recent research has shown that these waveforms do not accurately replicate the loading patterns experienced in pavement structures under various axle configurations [15–18]. Therefore, it is recommended to use real strain waveforms generated by different axle types—such as tandem and tridem axles—to more effectively assess the fatigue characteristics of asphalt mixtures [19,20]. The rest period refers to the unloading time between two successive loading pulses and is intended to capture the healing effects that occur during this phase. Rest periods typically range from 0.1 to over 5 s. Studies have shown that incorporating rest periods can significantly improve the fatigue life of the mixture by allowing for damage healing during unloading [21,22].

The previous discussion highlights that the fatigue responses of asphalt mixtures are closely influenced by temperature, strain waveforms, and rest periods. This complexity makes the analysis and interpretation of fatigue data highly challenging. Phenomenological fatigue analysis methods often struggle to yield consistent results across different testing conditions. As a result, researchers have typically relied on fatigue models tailored to specific loading conditions. To address this issue, the dissipated energy (DE) approach has been introduced to simplify fatigue data analysis [23,24]. DE represents the area enclosed by the stress–strain loop during each loading cycle, offering valuable insight into the mechanisms of fatigue damage from an energy perspective. Studies have demonstrated that DE is effective in developing unified fatigue models that describe asphalt mixture behavior across varying temperatures and loading levels. This allows for a more fundamental assessment of fatigue performance, which is less dependent on specific loading conditions [25,26].

Although the DE indicator shows significant potential for developing unified fatigue models and revealing fatigue damage in asphalt mixtures, its applicability needs further validation across a broader range of loading conditions, especially those involving more varied strain waveforms and rest periods. This necessity arises because most existing research on the DE indicator has relied on fatigue data obtained using conventional haversine or sinusoidal waveforms, rather than actual strain waveforms that better reflect field conditions. Furthermore, the influence of rest periods on the DE-fatigue behavior correlation has been largely unexplored. To address these gaps, this study aims to analyze the fatigue behaviors of asphalt mixtures subjected to a wide range of strain waveforms, temperatures, and rest periods using the dissipated energy approach. First, fatigue response data were

collected for asphalt mixtures exposed to three real strain waveforms, three temperature levels, and four different rest periods. Next, the effects of these three factors (strain waveform, temperature, and rest period) on asphalt mixture fatigue were analyzed using both conventional phenomenological methods and the DE method. Finally, based on the analysis results, a unified fatigue model was developed using the DE indicator to characterize the fatigue performance of asphalt mixtures across various conditions. The results of this study are expected to improve the assessment of fatigue behaviors and mechanisms in asphalt mixtures, providing valuable insights for better pavement structure design and asphalt material development.

2. Fatigue Test and Dissipated Energy Method

2.1. Materials and Specimens

A type of hot-mixed asphalt mixture, known as AC-13, was used for the investigation in this study. The AC-13 mixture employed a dense gradation, with its gradation curve shown in Figure 1. The mixture was prepared using a 60/70 penetration-grade base asphalt binder. The AC-13 asphalt mixture was designed according to the JTG F40 specifications [27] using the Marshall method. The optimal asphalt content was determined as 4.5%. Once the asphalt content was adopted, the average air voids of the mixture were measured at 3.96%, which aligns with the specification's requirements. The voids in mineral aggregate (VMA) of asphalt mixture was 14.7%, while the voids filled with asphalt (VFA) of the mixture was 73.1%. The mixture's bulk density was measured at 2.472 g/cm^3. The AC-13 mixture was designed following the Marshall method, achieving a Marshall stability of 11.2 kN.

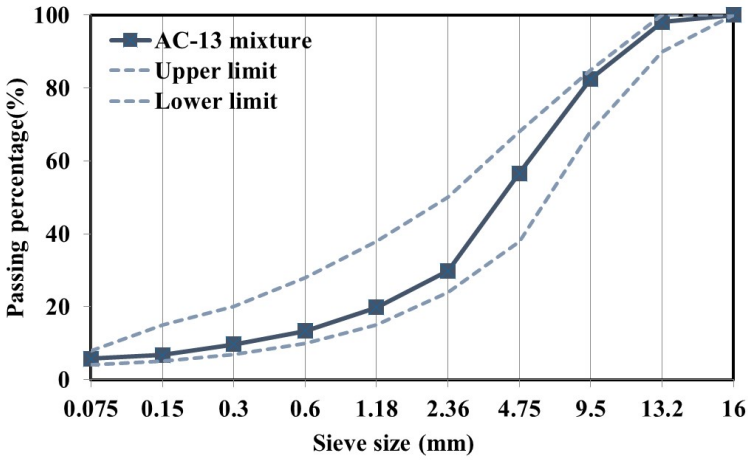


Figure 1. The curve of aggregate gradation of AC-13 mixture.

For the fatigue tests, hot-mixed AC-13 asphalt was prepared into beam specimens. First, the asphalt mixture was formed into slabs through roller compaction. Subsequently, the slabs were then cut into individual beam specimens using a saw. The final dimensions of each beam specimen were 380 mm × 50 mm × 63.5 mm. Photographs of the prepared specimens used for fatigue tests are shown in Figure 2.

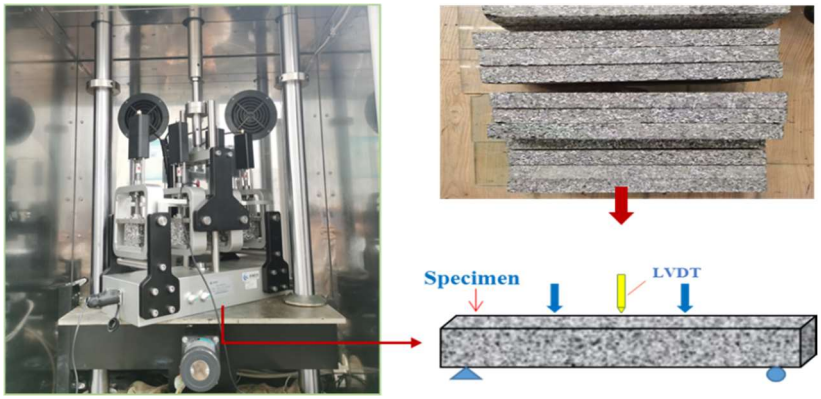


Figure 2. The loading setup and specimens used in 4PB fatigue test.

2.2. Fatigue Test Setup

In this research, the four-point bending (4PB) fatigue test was employed for measuring fatigue responses of asphalt mixture specimens. The diagrams of the testing apparatus and loading mode are depicted in Figure 2. As depicted, a linear variable differential transducer (LVDT) was employed to record the deflection of the specimen during the loading process. Using the applied force and measured deflection data, key fatigue response parameters—including strain magnitude, stiffness modulus—were determined.

Three types of strain waveforms were incorporated into fatigue tests to assess the effects of strain pulses on the mixture's fatigue behavior. These waveforms correspond to the actual strain response pulses experienced within the asphalt layer, generated by single-axle, tandem-axle, and tridem-axle configurations, respectively. Accordingly, they are referred to as the single-axle waveform, tandem-axle waveform, and tridem-axle waveform in this study. The detailed shapes of the three strain waveforms are shown in Figure 3. Three types of strain waveforms were identified based on field-measured strain data and finite element modeling of a flexible pavement structure [28]. The pavement consists of a 30 cm thick asphalt mixture layer, a 35 cm granular base layer, and a 20 cm subbase layer over subgrade. It is noteworthy that this pavement is an experimental setup, equipped with strain sensors to measure the strain responses of the pavement structure. To eliminate the potential impact of varying asphalt mixture types on pavement responses, a single asphalt mixture (i.e., AC-13) was used to construct the entire asphalt layer. The strain waveforms represent the transverse strain pulses at the bottom of the asphalt layer under three types of axle loads. Once the shapes of the loading waveforms were identified, they were programmed into the universal testing machine (UTM) using a template file. Subsequently, the UTM was able to apply the prescribed loading pulses to the specimen. Comparisons of the applied stress pulses are presented in Figure 3d.

It is seen that the tandem- and tridem-axle waveforms exhibit multiple peaks compared to the single-axle waveform. This is due to the strain superposition effect caused by the multiple axles, which leads to cumulative strain within asphalt layer [28]. Because of this superposition phenomenon, the overall duration of strain waveform increases with the number of axles. Specifically, the duration of the single-axle waveform was set to 0.1 s, corresponding to a loading frequency of 10 Hz. The tandem-axle and tridem-axle waveforms had durations of 0.132 s (corresponding to a frequency of 7.58 Hz) and 0.170 s (corresponding to a frequency of 5.88 Hz), respectively.

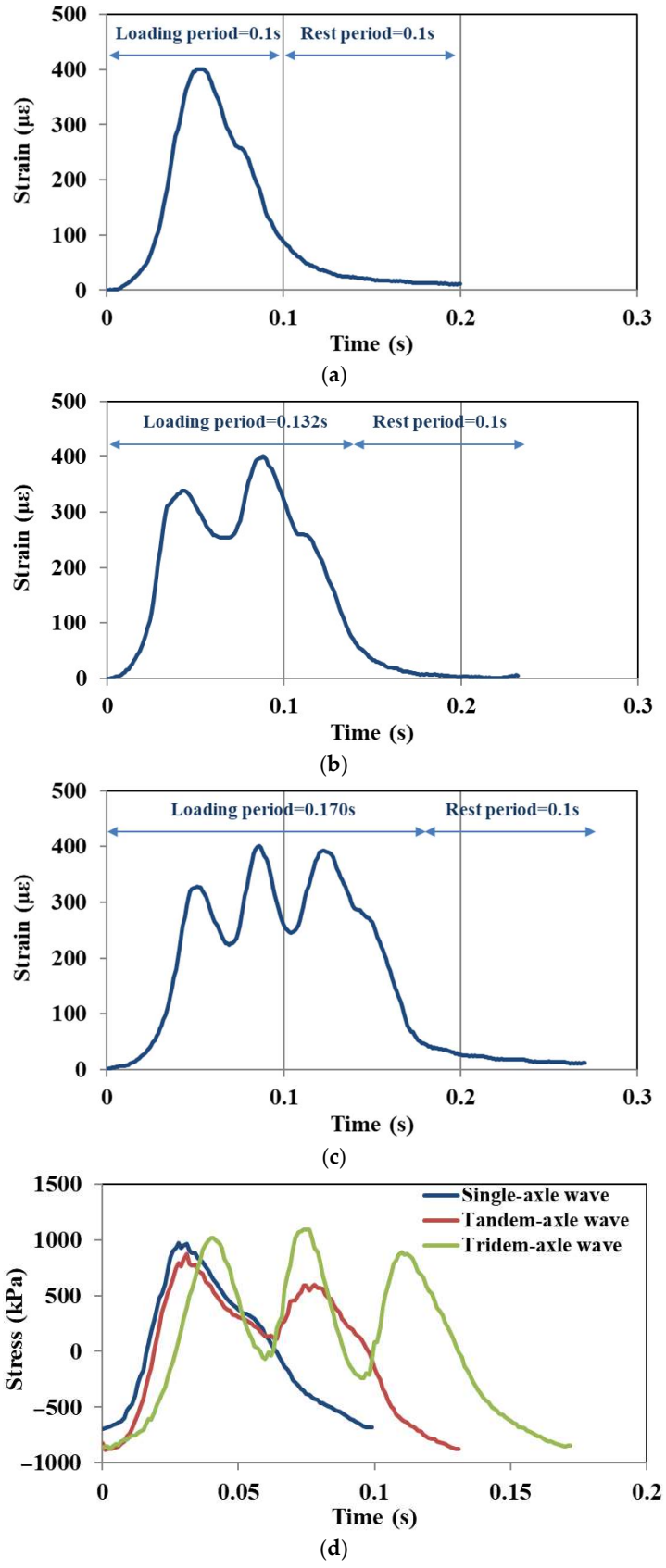


Figure 3. Three loading waveforms in 4PB test: (**a**) single-axle strain wave, (**b**) tandem-axle strain wave, (**c**) tridem-axle strain wave and (**d**) comparisons of three stress waveforms.

To investigate healing effects of rest periods on fatigue damage within asphalt mixture, four different rest period durations were considered in the fatigue tests, which were 0 s, 0.1 s, 0.5 s, and 1.0 s. The diagrams of three strain waveforms combined with a 0.1 s rest period are also presented in Figure 3. During the rest phase, the asphalt mixture undergoes strain recovery, returning to approximately a zero-strain state. In addition to strain waveform and rest period variations, different testing temperatures were also incorporated in this study: 20 °C, 10 °C, and 0 °C.

The 4PB tests followed a displacement-controlled pattern, where the displacement of the loading actuator remained constant throughout the loading process. Under this loading mode, the specimen's tensile strain gradually increased as the number of loading cycles increased. For consistency, the tensile strain recorded at the 50th loading cycle was designated as the initial strain level. This strain level refers to the maximum peak strain value in the single-axle or multi-axle strain pulse. Across different testing conditions, the initial applied strain levels ranged from 400 με to 1100 με. This manuscript aims to evaluate the fatigue performance of asphalt mixtures under varying temperatures and rest periods. As a result, the applied strain levels spanned a wide range to adjust to varying fatigue properties of asphalt mixture. At higher temperatures or longer rest periods, the fatigue life of the asphalt mixture could be extremely long if the applied strain level was low. Consequently, the maximum strain level in the fatigue tests was capped at 1000 με to optimize testing time. Under each loading scenario, two to six parallel specimens were tested to lower variability of testing results. During the fatigue test, the modulus of the mixture was calculated as the ratio of the stress pulse magnitude to the strain pulse magnitude. The fatigue life of the asphalt mixture was determined using the 50% stiffness reduction criterion, that is, the loading cycle at which the sample's modulus decreased to 50% of its initial value was defined as the fatigue life. Additionally, the tandem- and tridem-axle waveforms, which contain multiple peaks, were counted as a single compound cycle, as they represent one fatigue loading event from the axle.

2.3. Dissipated Energy Method

Dissipated energy (DE) is commonly utilized to analyze fatigue damage mechanisms of materials from an energy perspective. DE is defined as the region of the hysteresis loop formed from applied stress and measured strain data during cyclic loading. In the field of asphalt mixtures, researchers commonly use three DE-based indicators to describe fatigue behavior: the initial DE (IDE), the sum DE, and the stable changing rate of DE [29–31]. The IDE is the dissipated energy measured during the early stages of fatigue loading (e.g., 50th or 100th cycle), whereas the sum DE represents a total of dissipated energy accumulated throughout all cycles. The stable changing rate of DE is defined as the variation rate of dissipated energy in relation to loading cycles during stable damage accumulation phase. Existing studies have demonstrated that DE-based indicators can establish consistent relationships with the mixture's fatigue life, independent of strain levels. Therefore, these indicators are considered effective in reflecting fundamental fatigue damage mechanisms of the mixture under repeated loadings.

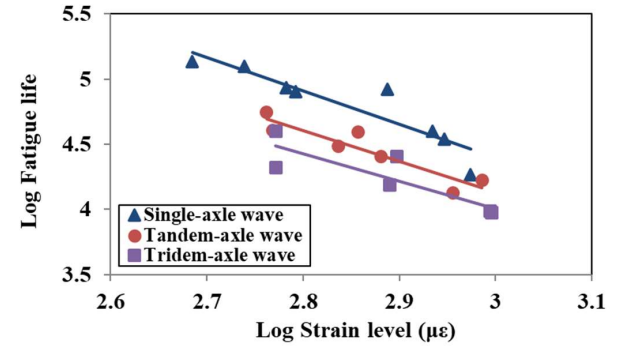
Although DE-based indicators have been widely applied, their uses have primarily focused on fatigue data obtained under simplified haversine or sinusoidal strain waveforms without rest periods. Their applicability for analyzing fatigue data measured under more realistic combinations of strain waveforms and temperatures, as well as rest periods, remains underexplored. In this study, the IDE indicator is employed for analyzing the fatigue characteristics of asphalt mixtures in extended loading scenarios, aiming at better characterizing the fatigue damage mechanisms of asphalt mixtures from an energy perspective.

3. Results and Discussion

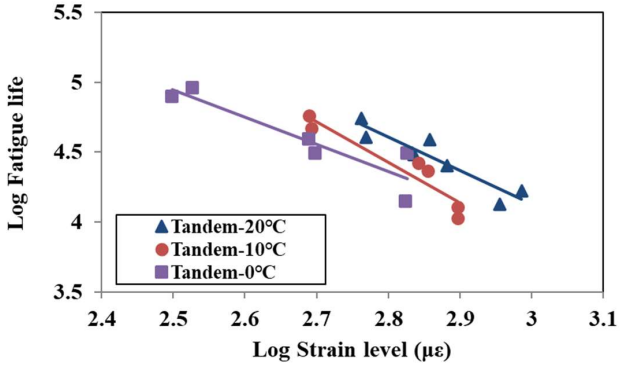
3.1. Comparisons of Fatigue Life Data Under Various Loading Scenarios Using Phenomenological Method

Fatigue responses of the asphalt mixture subjected to varying strain waveforms, strain levels, temperatures, and rest periods were obtained from the 4PB fatigue tests and are presented in Figure 4. As shown, the mixture's fatigue life evidently relies on different loading conditions. In particular, the fatigue life decreases as the strain level increases, implying that higher loading magnitudes accelerate fatigue damage within the material. A clear linear trend between fatigue life and strain level is observed on the dual log scale, independent of waveform type and temperature, as well as rest period, which aligns with observations reported in previous studies [32–35]. The relationships between fatigue life and strain levels were developed based on data shown in Figure 4 and are summarized in Table 1. It is seen that the correlation coefficients of the fitted models generally exceed 0.7, indicating a strong linear correlation between the fatigue life of the mixture and the strain level on a logarithmic scale.

Impacts of strain waveforms on fatigue life are pronounced as well, as depicted in Figure 4a. When strain level keeps the same, specimens subjected to a single-axle waveform exhibit the longest fatigue life, followed by those under a tandem-axle waveform, with a tridem-axle waveform resulting in the shortest fatigue life. The fatigue life of the mixture under a single-axle load is approximately three times longer than under a tandem-axle load, and about 4.5 times longer than under a tridem-axle load. This outcome is primarily attributed to differences in loading durations associated with the three waveform types. As discussed in Section 2.1, tandem-axle and tridem-axle waveforms, representing multiple-axle loadings, have extended loading durations compared to the single-axle waveform. Consequently, multi-axle loadings contribute to greater damage in asphalt mixture, reducing the mixture's fatigue life compared to the single-axle loading.

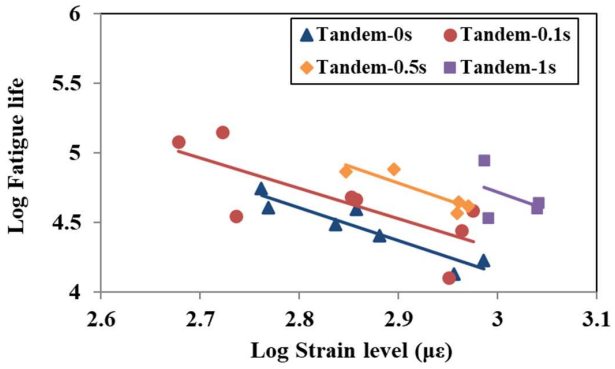


(a)



(b)

Figure 4. *Cont.*



(c)

Figure 4. Comparisons of fatigue life of asphalt mixture under diverse (**a**) strain waveforms, (**b**) temperatures and (**c**) rest periods.

Table 1. Fitting results of relationships between fatigue life and strain levels shown in Figure 4.

Figures	Cases	Fitting Results
Figure 4a	Single-axle wave	$N_f = 1.33 \times 10^{12} \cdot \varepsilon^{-2.58}$ $(R^2 = 0.84)$
	Tandem-axle wave	$N_f = 1.88 \times 10^{11} \cdot \varepsilon^{-2.38}$ $(R^2 = 0.86)$
	Tridem-axle wave	$N_f = 2.21 \times 10^{10} \cdot \varepsilon^{-2.11}$ $(R^2 = 0.74)$
Figure 4b	Tandem-20 °C (i.e., Single-axle case in Figure 4a)	$N_f = 1.88 \times 10^{11} \cdot \varepsilon^{-2.38}$ $(R^2 = 0.86)$
	Tandem-10 °C	$N_f = 3.18 \times 10^{12} \cdot \varepsilon^{-2.88}$ $(R^2 = 0.90)$
	Tandem-0 °C	$N_f = 6.24 \times 10^{9} \cdot \varepsilon^{-1.94}$ $(R^2 = 0.84)$
Figure 4c	Tandem-0 s (i.e., Single-axle case in Figure 4a)	$N_f = 1.88 \times 10^{11} \cdot \varepsilon^{-2.38}$ $(R^2 = 0.86)$
	Tandem-0.1 s	$N_f = 6.98 \times 10^{10} \cdot \varepsilon^{-2.18}$ $(R^2 = 0.58)$
	Tandem-0.5 s	$N_f = 9.33 \times 10^{11} \cdot \varepsilon^{-2.48}$ $(R^2 = 0.82)$
	Tandem-1 s	$N_f = 1.53 \times 10^{12} \cdot \varepsilon^{-2.49}$ $(R^2 = 0.68)$

Temperature plays a significant role in affecting fatigue life as well. As depicted in Figure 4b, higher temperatures result in an enhancement in fatigue resistance when the strain level remains constant. This behavior can be attributed to the viscoelastic characteristics of asphalt materials: with increasing temperature, the mixture's ability to deform enhances, thereby improving its ability to resist fatigue damage. Notably, fatigue data in Figure 4b were obtained under tandem-axle waveform loading. Single- and tridem-axle waveform testing results exhibit similar trends but are omitted here for brevity.

Rest periods also show noticeable impacts on the mixture's fatigue life, as illustrated in Figure 4c. At a constant strain level, fatigue life increases as the rest period grows from 0 s to 1 s. These findings indicate that incorporating a rest interval between loading cycles facilitates the healing of fatigue-induced damage within the material. Moreover, longer rest periods further amplify this healing effect, resulting in a more substantial improvement in fatigue life. This observation suggests that the role of rest periods should be carefully considered when developing fatigue models for asphalt mixtures. Another point to note is that the fitting correlation coefficient for the fatigue testing results, when considering rest periods, is relatively low compared to other loading scenarios. This indicates that further testing, incorporating additional rest period conditions, is necessary to enhance the reliability of the analysis.

3.2. Typical Stress–Strain Loops and DE Variation Patterns

The analysis in the previous section highlighted the significant impacts of waveform type on fatigue life. This section will focus on examining the stress–strain loops generated by different strain waveforms, with the goal of calculating the mixture's dissipated energy (DE) during fatigue loading. Additionally, the changes in DE as loading cycles increase will be evaluated to further understand how strain waveforms influence asphalt mixture fatigue from an energy dissipation perspective.

In this study, the raw stress and strain data of the asphalt mixture were recorded during the fatigue tests at a sampling interval of 0.001 s. Based on these raw data, stress–strain loops corresponding to different strain waveforms were constructed. Figure 5 compares stress–strain loops of the asphalt mixture under single-axle, tandem-axle, and tridem-axle waves. The shape of the stress–strain loop is influenced by the type of strain waveform. The loop generated by the single-axle wave is roughly oval-shaped, whereas the loops from the tandem-axle and tridem-axle tests are more irregular and feature overlapping regions. The overlapping regions result from the multiple peaks in the tandem-axle and tridem-axle strain waveforms. Due to these shape differences, the areas of the loops at each waveform vary depending on the strain waveform, which in turn leads to different DE values for the specimens. In addition, the tandem- and tridem-axle waves produce elevated DE in the asphalt mixture compared to the single-axle wave. This observation helps explain why mixtures subjected to multi-axle waveforms typically exhibit shorter fatigue life compared to those subjected to single-axle loading.

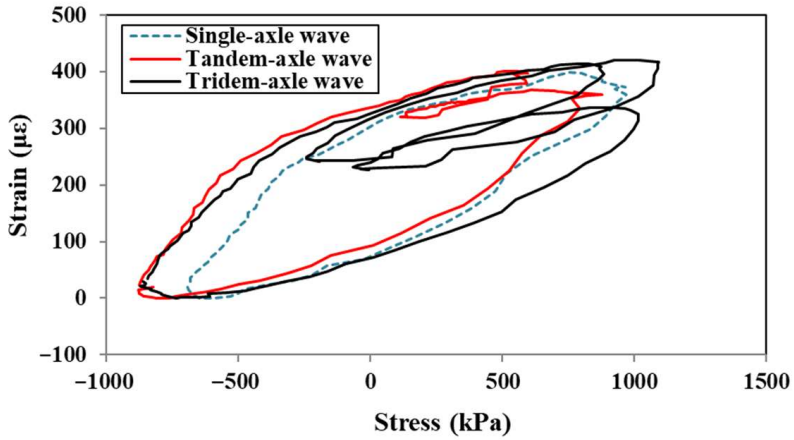
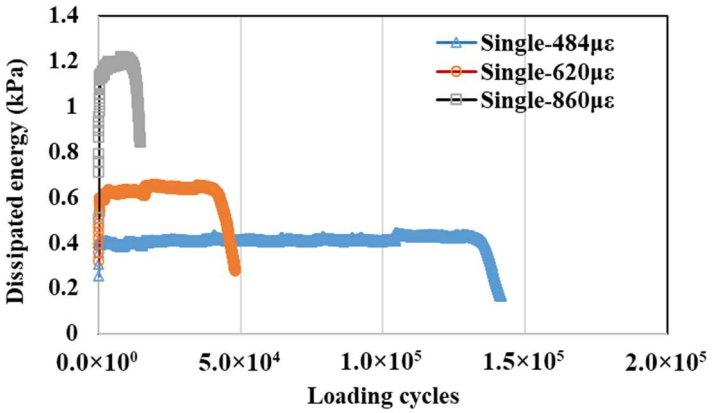
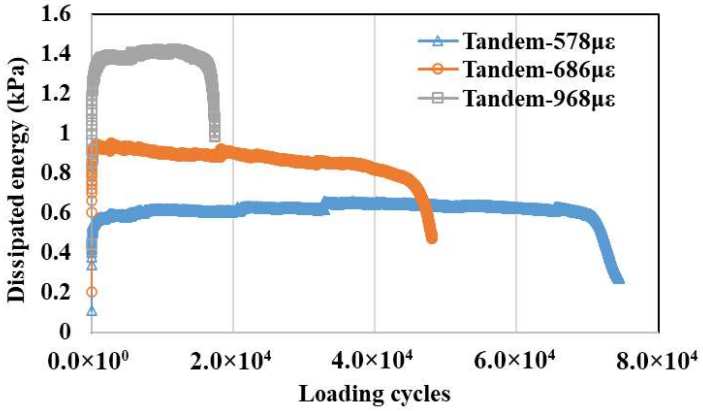


Figure 5. Comparisons of stress–strain loops generated from three strain waveforms.

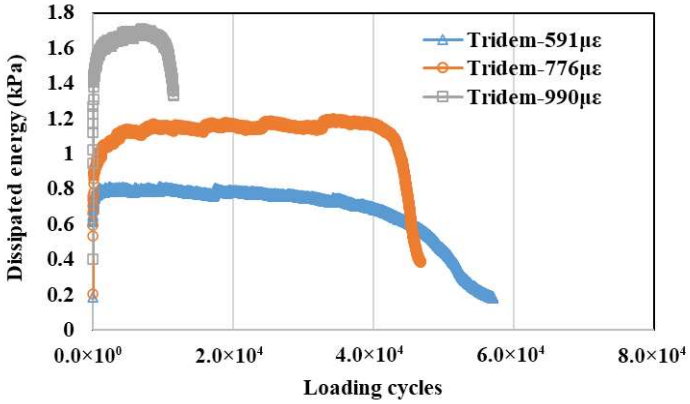
The dissipated energy (DE) was subsequently calculated as the area enclosed by each stress–strain loop, which was then used to construct the variation patterns of DE throughout the fatigue loading process. For the test data with rest periods, only the stress and strain data from the loading phase were used to construct the stress–strain loops and calculate the dissipated energy, while the data from the unloading (i.e., rest) phase were excluded. This approach was adopted because energy dissipation primarily occurs during the fatigue loading stage. The typical DE variation curves with respect to loading cycles, measured for each of the three strain waveforms, are presented in Figure 6.



(**a**)



(**b**)



(**c**)

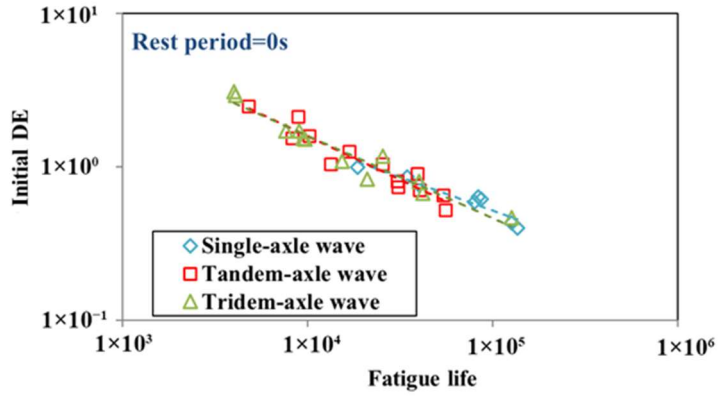
Figure 6. Variation curves of DEs with loading cycles in (**a**) single-axle wave tests, (**b**) tandem-axle wave tests, and (**c**) tridem-axle wave tests.

As illustrated in Figure 6, the DE values follow a distinct pattern across three phases as the loading cycles progress, regardless of strain levels or strain waveform types. In Phase I, the DE climbs quickly with the rise in loading repetitions, indicating that the initial stages of fatigue loading lead to a rapid accumulation of damage in the material. In Phase II, DE continues to rise but at a slower and more stable rate compared to Phase I, suggesting that the asphalt mixture undergoes moderate damage accumulation during this phase. In Phase III, the DE sharply declines as the loading cycles increase, continuing until fatigue cracking occurs in the asphalt mixture. This decline may be attributed to the significant reduction in stiffness modulus when the test approaches the end, which results in narrower stress–strain loops, and consequently, lower DE values.

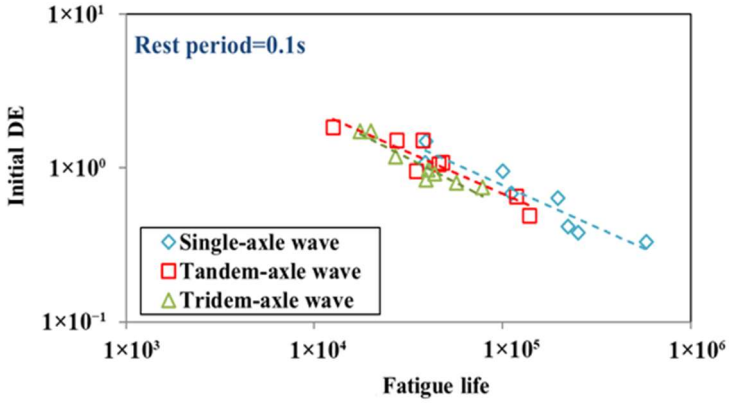
Additionally, it was observed that the variation patterns of DE are influenced by strain levels and strain waveforms. Specifically, the DE exhibits more rapid changes at higher strain levels and under multi-axle waveforms, indicating that both high strain levels and multi-axle loadings accelerate the accumulation of fatigue damage within the material. The initial DE generated by the tandem-axle wave is approximately 1.3 times that generated by the single-axle wave, while the DE generated by the tridem-axle wave is about 2.0 times that of the single-axle wave. This observation is consistent with the comparison of fatigue lives in different conditions, further supporting the potential of the DE indicator to reflect the mixture's fatigue life. A detailed analysis of the correlation between DE and fatigue life will be presented in the following sections.

3.3. The Effects of Strain Waveforms on the IDE vs. Fatigue Life Relationships

The findings in Section 3.2 suggest that the DE indicator holds promise in accurately reflecting the mixture's fatigue life. To further assess this hypothesis, Figure 7 shows the correlation between the initial dissipated energy (IDE) and the fatigue life at various strain waveforms and rest periods. For comparison purposes, a unified criterion was adopted to determine the IDE value: IDE was defined as the dissipated energy (DE) corresponding to the 50th loading cycle. It also should be noted that the test temperature for the data shown in Figure 7 is 20 °C.



(**a**)



(**b**)

Figure 7. *Cont.*

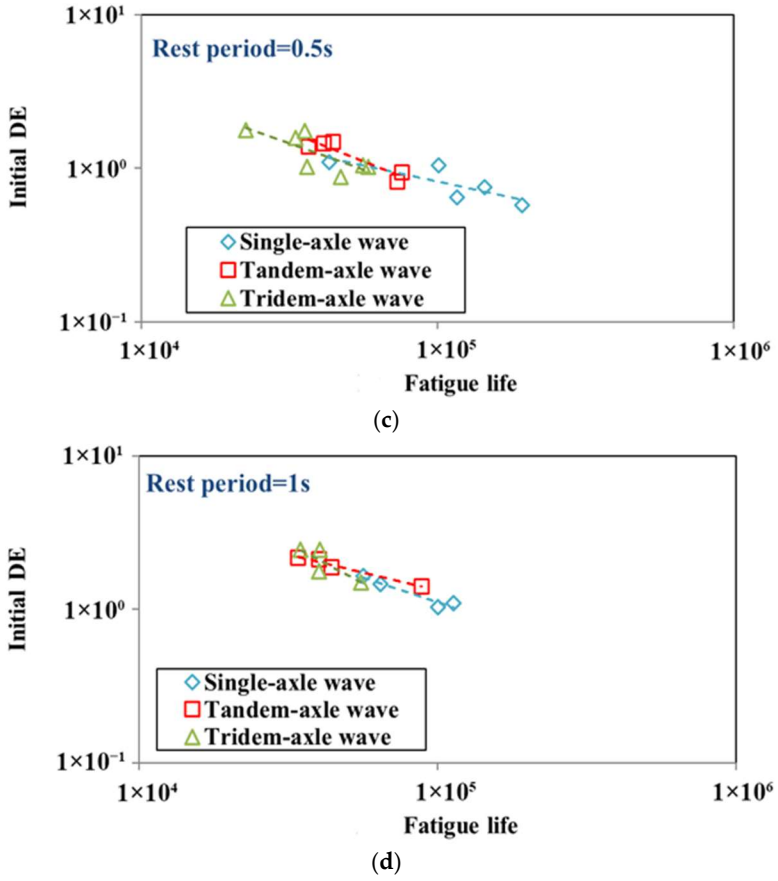


Figure 7. The relationships between IDE and fatigue life under three strain waveforms with rest periods of (**a**) 0 s, (**b**) 0.1 s, (**c**) 0.5 s, and (**d**) 1 s.

As shown in Figure 7a, fatigue life of the specimen shows an approximately linear correlation with the IDE value on the dual log scale, irrespective of the strain waveform used. An increase in IDE corresponds to a reduction in fatigue life, indicating that the IDE indicator is closely related to the mixture's fatigue life. Moreover, the fatigue life trends in relation to IDE from the three different strain waveforms align closely with one another, regardless of the rest periods. This consistency suggests that the correlation between IDE and fatigue life is universal, unaffected by the type of strain waveform. Consequently, using the IDE indicator proves useful for developing a generalized model to describe fatigue behavior under various strain waveform conditions.

As shown in Figure 7b–d, similar patterns are observed when different rest periods are applied. Specifically, fatigue life decreases almost linearly with increasing IDE, and this trend remains consistent regardless of the strain waveform or rest period. Thus, 4PB fatigue testing results further confirm that the IDE-fatigue life correlation is unaffected by strain waveforms, even with varying rest periods.

3.4. The Effects of Temperatures on the IDE vs. Fatigue Life Relationships

In addition to strain waveform, the effects of temperature on the IDE-fatigue life relationship were also examined in this study. As seen from Figure 8, the mixture's fatigue life demonstrates a strong linear relationship with the IDE on the double logarithmic scale at other temperatures (i.e., 0 °C and 10 °C). However, the temperature's effect on this linear relationship is less pronounced. The IDE-fatigue lifeline at 20 °C lies above the line at 10 °C, and similarly, the line at 0 °C is positioned above that at 10 °C. This suggests that

temperature may influence the IDE-fatigue life relationship, but the trends are somewhat ambiguous and require further investigation for a clearer understanding.

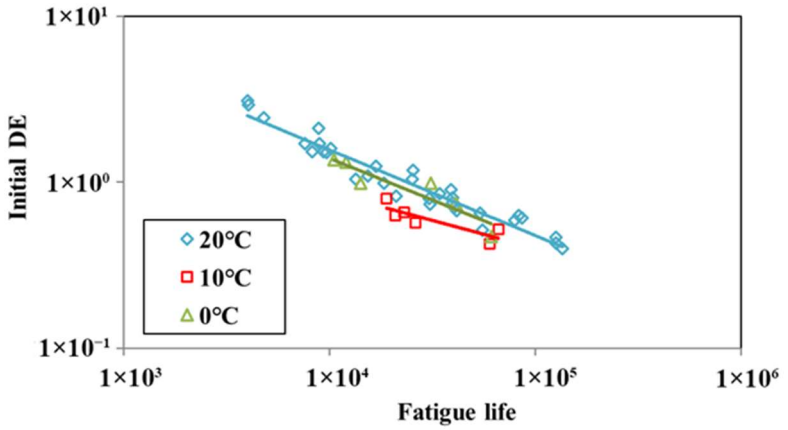


Figure 8. Correlations between IDE and fatigue life measured at different temperatures.

3.5. The Effects of Rest Periods on the IDE vs. Fatigue Life Relationships

The previous section's discussions indicate that the IDE-fatigue life relationship remains unaffected by the strain waveforms, whether or not a rest period is included. However, it was observed that the relationship is influenced by the rest period. Figure 9 presents IDE values in relation to fatigue life under different rest period durations. Since the impact of temperature on the IDE-fatigue life relationship is not very clear, all the fatigue data in Figure 9 are based on an unchanged temperature of 20 °C for consistency in comparison.

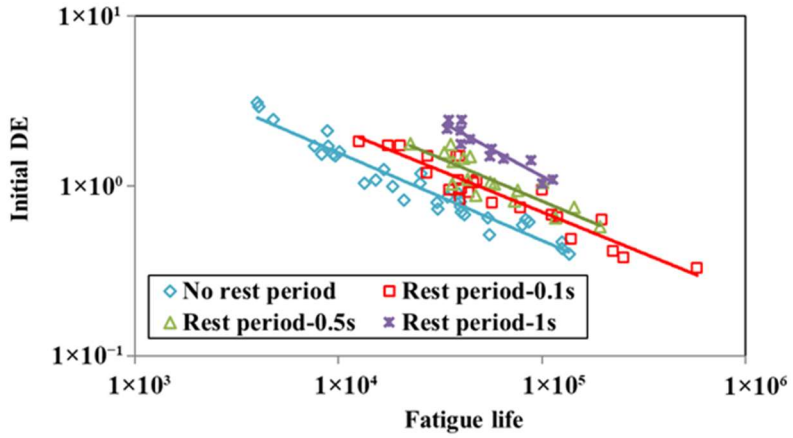


Figure 9. The relationships between IDE and fatigue life under different rest periods.

As shown in Figure 9, there are clear differences in the IDE-fatigue life relationships across different rest period durations. Specifically, as rest period increases, the IDE-fatigue life curve shifts upward, almost in parallel. This indicates that a higher rest period results in greater fatigue life for asphalt mixture specimen. Consequently, the rest period significantly influences how fatigue life changes with IDE. It can be challenging to develop a single, universal IDE-fatigue life curve that fits all rest period durations. This variation in the IDE-fatigue life relationship is likely caused by the healing effects of rest periods. With a constant IDE, the extending rest period allows the asphalt mixture to recover from some of its fatigue damage, thereby increasing its fatigue life. As a result, the IDE-fatigue life curve shifts toward higher fatigue life values. The differences between these curves reflect the varying degrees of healing effects for each rest period.

A fatigue model, as shown in Equation (1), was proposed in this research to describe the IDE-fatigue life relationship across different rest periods. Based on data in Figure 9, the model was developed and the fitting correlation coefficients were shown as Equation (2). For comparison, the predicted fatigue lives based on IDE and rest period are plotted against the measured fatigue lives in Figure 10.

$$N_f = a \cdot e^{b \cdot RP} \cdot IDE^c \quad (1)$$

$$N_f = 20963.73 \cdot e^{1.93RP} \cdot IDE^{-2.58} \quad (R^2 = 0.917) \quad (2)$$

where N_f is the fatigue life, RP is the rest period, IDE is the initial dissipated energy, and a, b and c are fitting parameters.

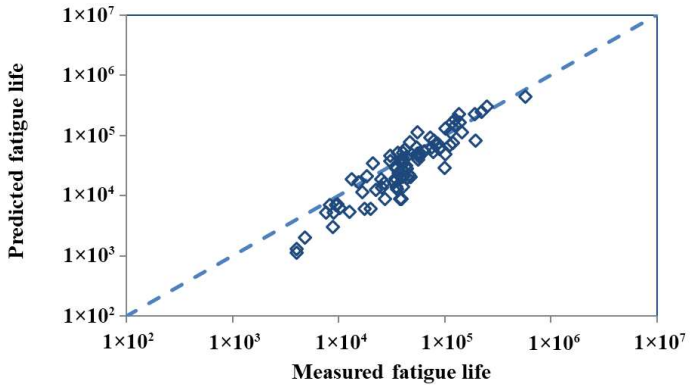


Figure 10. Comparisons of the predicted fatigue life and the measured fatigue life.

From Equation (2), it is evident that the model is effective, with a strong fitting correlation coefficient of 0.917. Figure 10 further demonstrates that the model provides reasonably accurate predictions of the mixture's fatigue life. Using this equation, the fatigue life of the specimen under various rest periods can be reliably predicted from its IDE, enabling the estimation of asphalt mixture fatigue life across various conditions with a single unified model. Notably, the IDE serves as a particularly useful indicator compared to other DE-related metrics, as it can be measured early in the fatigue test, thus offering a significant reduction in test duration. It is noteworthy that the fitting accuracy of Equation (1) was only validated via data in this research. The applicability of this equation still needs verification via data tested on more asphalt mixtures.

4. Conclusions

This research analyzes the fatigue behaviors of asphalt mixtures under extended combinations of strain waveforms, temperatures, and rest periods with dissipated energy approach. From the findings, the following conclusions can be drawn.

(1) All three factors—strain waveforms, temperatures, and rest periods—significantly influence the fatigue life of asphalt mixtures. Specifically, the multi-axle waveform produces a shorter fatigue life in comparison with the single-axle waveform due to longer loading durations. The fatigue life of the mixture under a single-axle load is approximately three times longer than under a tandem-axle load, and about 4.5 times longer than under a tridem-axle load. In contrast, both increased temperature and longer rest periods contribute to a longer fatigue life, highlighting the role of viscoelastic properties and healing effects in asphalt mixture fatigue.

(2) The shape of the stress–strain hysteresis loop in asphalt mixtures is affected by the type of strain waveform, resulting in variations in dissipated energy (DE) values. The DE values exhibit a distinct progression across three phases as loading cycles advance. These

variation patterns are influenced by both strain levels and strain waveforms. Notably, the initial DE generated by the tandem-axle wave is approximately 1.3 times that generated by the single-axle wave, while the DE generated by the tridem-axle wave is about 2.0 times that of the single-axle wave. DE values change more rapidly at higher strain levels and under multi-axle waveforms, suggesting that both high strain and multi-axle loading accelerate the accumulation of fatigue damage.

(3) The initial DE (IDE) indicator promises to be an effective tool for understanding the fatigue behavior of asphalt mixtures in terms of energy. IDE establishes a unique relationship with the fatigue life of asphalt mixtures that is unaffected by strain levels and strain waveforms. Nevertheless, the IDE-fatigue life correlation is affected by rest periods and temperatures. Increasing the rest period shifts the IDE-fatigue life curve toward longer fatigue life, while the effect of temperature remains unclear and requires further investigation.

(4) Based on IDE analysis, a model was developed to describe the IDE-fatigue life relationship across a broad range of strain waveforms, strain levels, and rest periods. This model demonstrates strong predictive capability, with a correlation coefficient of 0.917. By applying this model, the fatigue life of asphalt mixtures under different loading conditions can be reliably estimated from their IDE, enabling consistent prediction of fatigue life across diverse scenarios using a unified model.

It is important to note that the results of this research were based on a specific asphalt mixture type (i.e., AC-13). Additional testing on a broader range of mixture types is needed to further validate the findings of this study. On the other hand, the results of this study were derived from laboratory-based fatigue testing. Field observations or full-scale pavement testing are therefore required to validate the present findings and further improve evaluation accuracy.

Another direction for future work concerns loading waveforms—in this study, the applied loading waveforms were limited to a specific pavement structure and three axle configurations. In contrast, in situ traffic loading encompasses a wide range of tire and axle configurations (e.g., quad axles), as well as varying traffic speeds. Consequently, additional research is needed to incorporate more realistic traffic loading conditions into fatigue evaluation, thereby ensuring that laboratory testing results more accurately reflect actual field performance.

Author Contributions: Conceptualization, Y.C. and H.C.; Methodology, Y.C. and H.C.; Validation, M.H.; Formal analysis, X.W. and H.C.; Investigation, Y.C., J.G. and M.H.; Resources, X.W., J.G. and L.S.; Writing—original draft, Y.C. and H.C.; Writing—review & editing, H.C.; Supervision, L.S. All authors have read and agreed to the published version of the manuscript.

Funding: This research was funded by the National Natural Science Foundation of China (Grant No. 52578527), the Key Engineering Science and Technology Project of Jiangxi Provincial Department of Transportation (2024ZG006), the Research Project of Hebei Transportation Investment Group Hengde Expressway Co (HD-202441) and the Fundamental Research Funds for the Central Universities.

Data Availability Statement: All data will be available on request to authors.

Acknowledgments: This work was supported by the National Natural Science Foundation of China (Grant No. 52578527), the Key Engineering Science and Technology Project of Jiangxi Provincial Department of Transportation (2024ZG006), the Research Project of Hebei Transportation Investment Group Hengde Expressway Co (HD-202441) and the Fundamental Research Funds for the Central Universities. The sponsorships are gratefully acknowledged.

Conflicts of Interest: Author Yu Cai was employed by the company Zhangji Expressway Reconstruction and Expansion Project Office of Jiangxi Provincial Transportation Investment Group Co., Ltd. Authors Xiangping Wang ans Jia Guo were employed by the company Hebei Transportation

Investment Group Hengde Expressway Co., Ltd. The remaining authors declare that the research was conducted in the absence of any commercial or financial relationships that could be construed as a potential conflict of interest.

References

1. Chen, X.; Wang, Y.; Wen, Y.; Cheng, H.; Hao, G.; Wang, J. Quantitative analysis of oxidative aging effects on the fatigue resistance of asphalt mixtures based on the simplified viscoelastic continuum damage (S-VECD) model. *Int. J. Fatigue* **2023**, *177*, 107916. [CrossRef]
2. Cheng, H.; Wang, Y.; Chong, D.; Xia, C.; Sun, L.; Liu, J.; Gao, K.; Yang, R.; Jin, T. Truck platooning reshapes greenhouse gas emissions of the integrated vehicle-road infrastructure system. *Nat. Commun.* **2023**, *14*, 4495. [CrossRef]
3. Al-Qadi, I.L.; Nassar, W.N. Fatigue shift factors to predict HMA performance. *Int. J. Pavement Eng.* **2003**, *4*, 69–76. [CrossRef]
4. Xiao, X.; Li, J.; Cai, D.; Cheng, H.; Xiao, F. Characterizing thermal fatigue behaviors of asphalt concrete waterproofing layer in high-speed railway using customized overlay test. *Int. J. Fatigue* **2022**, *165*, 107176. [CrossRef]
5. Mansourkhaki, A.; Sarkar, A. Fatigue Performance of Asphalt Mixture under Actual Loading Patterns at Different Pulse Durations. *J. Test. Eval.* **2015**, *43*, 867–877. [CrossRef]
6. Tian, T.; Jiang, Y.; Yi, Y.; Nie, C. The splitting fatigue properties of ultra-large particle size asphalt mixture under the coupling effect of temperature and load. *Eng. Fract. Mech.* **2025**, *319*, 110990. [CrossRef]
7. Cubilla, D.; Gulisano, F.; Apaza, F.R.A.; Boada-Parra, G.; Gallego, J. Instantaneous and long-term piezoresistive response of asphalt mixtures with carbon fibers under dynamic flexural fatigue testing. *Constr. Build. Mater.* **2025**, *491*, 142646. [CrossRef]
8. Cheng, H.; Liu, J.; Sun, L.; Liu, L.; Zhang, Y. Fatigue behaviours of asphalt mixture at different temperatures in four-point bending and indirect tensile fatigue tests. *Constr. Build. Mater.* **2021**, *273*, 121675. [CrossRef]
9. Lv, S.; Xia, C.; Liu, C.; Zheng, J.; Zhang, F. Fatigue equation for asphalt mixture under low temperature and low loading frequency conditions. *Constr. Build. Mater.* **2019**, *211*, 1085–1093. [CrossRef]
10. Kutay, M.E.; Lanotte, M. Viscoelastic continuum damage (VECD) models for cracking problems in asphalt mixtures. *Int. J. Pavement Eng.* **2018**, *19*, 231–242. [CrossRef]
11. Sabouri, M.; Kim, Y.R. Development of a failure criterion for asphalt mixtures under different modes of fatigue loading. *Transp. Res. Rec. J. Transp. Res. Board* **2014**, *2447*, 117–125. [CrossRef]
12. Wei, H.; Xu, B.; Li, J.; Zheng, J.; Liu, Y.; Lu, R. Effect of temperature on fatigue damage evolution of asphalt mixture based on cluster analysis and acoustic emission parameters. *Eng. Fract. Mech.* **2025**, *317*, 110954. [CrossRef]
13. Al-Khateeb, G.G.; Ghuzlan, K.A. The combined effect of loading frequency, temperature, and stress level on the fatigue life of asphalt paving mixtures using the IDT test configuration. *Int. J. Fatigue* **2014**, *59*, 254–261. [CrossRef]
14. Wang, W.; Cheng, H.; Sun, L.; Sun, Y.; Liu, N. Multi-performance evaluation of recycled warm-mix asphalt mixtures with high reclaimed asphalt pavement contents. *J. Clean. Prod.* **2022**, *377*, 134209. [CrossRef]
15. Cheng, H.; Sun, L.; Wang, Y.; Chen, X. Effects of actual loading waveforms on the fatigue behaviours of asphalt mixtures. *Int. J. Fatigue* **2021**, *151*, 106386. [CrossRef]
16. Cheng, H.; Sun, L.; Wang, Y.; Chen, X. Analysis of fatigue behaviors of asphalt mixture under actual loading waveforms using pseudo-strain-based approaches. *Int. J. Pavement Eng.* **2023**, *24*, 2020269. [CrossRef]
17. Chatti, K.; El Mohtar, C.S. Effect of different axle configurations on fatigue life of asphalt concrete mixture. *Transp. Res. Rec. J. Transp. Res. Board* **2004**, *1891*, 121–130. [CrossRef]
18. Chatti, K.; Manik, A.; Brake, N.; Salama, H.; Haider, S.W. *Effect of Michigan Multi-Axle Trucks on Pavement Distress*; MDOT Final report; Michigan State University: East Lansing, MI, USA, 2009; Volume III.
19. Homsi, F.; Bodin, D.; Yotte, S.; Breysse, D.; Balay, J.M. Fatigue life modelling of asphalt pavements under multiple-axle loadings. *Road Mater. Pavement Des.* **2012**, *13*, 749–768. [CrossRef]
20. Homsi, F.; Bodin, D.; Yotte, S.; Breysse, D.; Ballay, J.-M. Multiple axle loadings: Shape parameters and their effect on the fatigue life of asphalt mixtures. *Eur. J. Environ. Civ. Eng.* **2011**, *15*, 743–758. [CrossRef]
21. Baaj, H.; Mikhailenko, P.; Almutairi, H.; Di Benedetto, H. Recovery of asphalt mixture stiffness during fatigue loading rest periods. *Constr. Build. Mater.* **2018**, *158*, 591–600. [CrossRef]
22. Ayar, P.; Moreno-Navarro, F.; Sol-Sánchez, M.; Rubio-Gámez, M.C. Exploring the recovery of fatigue damage in bituminous mixtures: The role of rest periods. *Mater. Struct.* **2018**, *51*, 25. [CrossRef]
23. Carpenter, S.H.; Shen, S. Dissipated energy approach to study hot-mix asphalt healing in fatigue. *Transp. Res. Rec. J. Transp. Res. Board* **2006**, *1970*, 178–185. [CrossRef]
24. Shen, S.; Airey, G.D.; Carpenter, S.H.; Huang, H. A dissipated energy approach to fatigue evaluation. *Road Mater. Pavement Des.* **2006**, *7*, 47–69. [CrossRef]
25. Shen, S.; Carpenter, S.H. Application of the dissipated energy concept in fatigue endurance limit testing. *Transp. Res. Rec. J. Transp. Res. Board* **2005**, *1929*, 165–173. [CrossRef]

26. Modarres, A.; Aloogar, A. Comparison between the fatigue response of hot and warm mix asphalts based on the dissipated energy approach. *Int. J. Pavement Eng.* **2017**, *18*, 60–72. [CrossRef]
27. *JTG D50—2017*; Specification for Construction of Highway Asphalt Pavement. Ministry of Transport of the People's Republic of China: Beijing, China, 2004.
28. Cheng, H.; Liu, L.; Sun, L.; Li, Y.; Hu, Y. Comparative analysis of strain-pulse-based loading frequencies for three types of asphalt pavements via field tests with moving truck axle loading. *Constr. Build. Mater.* **2020**, *247*, 118519. [CrossRef]
29. Ameri, M.; Seif, M.; Abbasi, M.; Molayem, M.; KhavandiKhiavi, A. Fatigue performance evaluation of modified asphalt binder using of dissipated energy approach. *Constr. Build. Mater.* **2017**, *136*, 184–191. [CrossRef]
30. Ghuzlan, K.A.; Carpenter, S.H. Fatigue damage analysis in asphalt concrete mixtures using the dissipated energy approach. *Can. J. Civ. Eng.* **2006**, *33*, 890–901. [CrossRef]
31. Bhasin, A.; Branco, V.T.C.; Masad, E.; Little, D.N. Quantitative comparison of energy methods to characterize fatigue in asphalt materials. *J. Mater. Civ. Eng.* **2009**, *21*, 83–92. [CrossRef]
32. Cheng, H.; Liu, J.; Sun, L.; Liu, L. Critical position of fatigue damage within asphalt pavement considering temperature and strain distribution. *Int. J. Pavement Eng.* **2021**, *22*, 1773–1784. [CrossRef]
33. Di Benedetto, H.; de La Roche, C.; Baaj, H.; Pronk, A.; Lundström, R. Fatigue of bituminous mixtures. *Mater. Struct.* **2004**, *37*, 202–216. [CrossRef]
34. Mateos, A.; Wu, R.; Denneman, E.; Harvey, J. Sine versus Haversine Displacement Waveform Comparison for Hot Mix Asphalt Four-Point Bending Fatigue Testing. *Transp. Res. Rec. J. Transp. Res. Board* **2018**, *2672*, 372–382. [CrossRef]
35. Zhang, Y.; Zhu, W.; Chu, X.; Dong, H.; Liu, D.; Liu, Y.; Chen, H.; Cheng, H.; Sun, L. Effect of design parameters on degree of blending and performance of recycled hot-mix asphalt incorporating fine reclaimed asphalt pavement particles. *J. Clean. Prod.* **2023**, *430*, 139708. [CrossRef]

Disclaimer/Publisher's Note: The statements, opinions and data contained in all publications are solely those of the individual author(s) and contributor(s) and not of MDPI and/or the editor(s). MDPI and/or the editor(s) disclaim responsibility for any injury to people or property resulting from any ideas, methods, instructions or products referred to in the content.